Mercury compounds characterization by thermal desorption

M. Rumayor, M. Diaz-Somoano, M. A. Lopez-Anton, M. R. Martinez-Tarazona

Instituto Nacional del Carbón (CSIC). C/ Francisco Pintado Fe Nº 26, 33011, Oviedo, Spain

**Corresponding author*

Phone: +34 985119090

Fax: +34 985297662

e-mail: mercedes@incar.csic.es

Abstract

The ability to accurately determine metal mercury content and identify different mercury species in solid samples is essential for developing remediation and control strategies. The aim of the present study is to characterize mercury compounds based on thermal desorption. For this purpose a series of samples was prepared and the operational parameters - heating velocity, carrier gas - were optimized. Fifteen commercial mercury compounds were analysed for use as fingerprints. The results of the study show that the identification of mercury species by the method of thermal desorption is possible. The temperature of desorption increased according to the following order HgI_2 < $HgBr_2$ < Hg_2Cl_2 = $HgCl_2$ < $Hg(CN)_2$ <$HgCl_2O_8{\cdot}H_2O$<$Hg(SCN)_2$<HgS (red) <HgF_2<$Hg_2(NO_3)_2{\cdot}2H2O$<$Hg(NO_3)_2{\cdot}H_2O$<HgO (yellow, red)<Hg_2SO_4<$HgSO_4$. A comparison of the estimated total mercury content with the mercury content calculated by integrating the area of the desorption curve shows that recoveries of 79-104 % for HgS can be estimated. The proposed method represents a significant step forward in direct mercury analysis in solid samples.

Keywords: Mercury speciation, solid samples, thermal desorption

1. Introduction

Mercury (Hg) species are potentially toxic compounds, having special concern for human health and the environment. Mercury enters the environment after being released from natural and anthropogenic sources [1]. Because Hg cycles, it can be carried over long distances far away from the source of its emission. It is then deposited in aquatic environments through precipitation and is generally found in organic form as methylmercury.

Mercury is rare in its native state. The main mercury ores include cinnabar and calomel, though there are a few other secondary minerals (corderoite, livingstonite…). Rocks, sediments, water, and soil, all contain small amounts of mercury, which may be released into the environment due to exposure to wind, water, and volcanic activity. However human activity has increased the mobilization and transformations of mercury into the environment [2]. Until now most attention has been directed towards the total amount of mercury. However the behaviour of Hg when it is emitted from different sources and its final fate and distribution in byproducts depend to a large extent on the form in which it occurs [3]. Each mercury species in a solid matrix interact in different ways, exhibiting a different degree of solubility and mobility. Moreover the development of mercury remediation and control technologies [3] must take into account mercury associations and the interaction of mercury with solids.

Sequential extraction procedures based on the different solubilities of Hg compounds are commonly used for Hg speciation studies [5-9]. These methods normally consist of several steps with one or more reagents, making the procedure both tedious and time consuming. Sample contamination or losses of mercury through volatilization are problems generally associated with these methods [10,11]. Other limitations are the

poor reproducibility and selectivity of the results. The advantages of these methods, however, are that they are quite easy to carry out in a standard laboratory and they are relatively cheap. As alternatives, instrumental methods such as X-ray adsorption fine structure spectroscopy (EXAFS) [12,13] and X-ray absorption near edge structure (XANES) [14], have been applied for mercury speciation in sediments and soils, but, these techniques are expensive and the detection limits (100 mg kg^{-1}) are not usually appropriate for the analysis of the majority of solid samples. Additionally, for decades, thermal desorption techniques have been applied for mercury speciation to a variety of solid samples such as sediments [15–21], iron-based sorbents for mercury removal [22], fluorescent lamp wastes [23], airborne particulate matter [24] and combustion power station by-products [25-27]. However reproducible results have still not been obtained, in part due to the lack of reference materials for validation purposes. To fill this gap, this study aims to characterize mercury compounds by their behaviour during thermal desorption. Although thermo-desorption is not a new technique the proposed application represents a significant step forward for mercury direct analysis in solid samples.

2. Materials and methods

For this study an advanced RA-915 Mercury analyzer coupled to a Pyro-915 furnace, both from Lumex, were used. This mercury analyzer is a highly versatile equipment that can be used to determine Hg contents in air, liquids and solids both in laboratory and field conditions. The operation of an RA-915 analyzer is based on differential Zeeman atomic absorption spectrometry using high frequency modulation of light polarization. The PYRO-915+ furnace consists of two chambers in series. The first one serves to evaporate liquids and pyrolyze the solid samples. In this section the mercury

compounds are released from the solid matrix under a controlled heating mode. The second chamber is kept at approximately 800°C and is used to reduce the mercury compounds to elemental mercury and to eliminate smoke and interference compounds. The temperature of the first chamber is continuously monitored by means of a thermocouple. Calibration coefficient is set using standard mercury-containing sample. A feature of the equipment is the high calibration stability.

For the purpose of the present study the heating mode was optimised until a good signal resolution was obtained. As can be seen in Table 1 a four-step program was set up. The temperature rate was kept at 40 ºC min^{-1} for 575 seconds. Then the heating velocity was increased up to 50 ºC min^{-1} where it was held for 200 seconds and then up to 80 ºC min^{-1} where it was held for a further 125 seconds. Air was used as carrier gas at 1 L min^{-1}.

In a first step commercial pure mercury compounds were analysed in order to determine their desorption temperature and profile. Because of the high Hg content the commercial pure compounds were previously diluted by blending them with an inert material. For this purpose 10 mg of each pure Hg compound was crushed and mixed with silica to obtain the fifteen standard homogenised samples with Hg concentrations of about 800 mg kg^{-1}. Each sample was analysed three times. The accuracy and precision of the analysis was determined by means of several analysis of a standard sample. HgS was selected for this evaluation. The Hg species were characterized by the temperature range in which they were released. The compounds tested were i) the most common mercury compounds found in coal and geological samples: $HgCl_2$, HgS, $HgSO_4$, HgO, Hg_2Cl_2, Hg_2SO_4, $HgBr_2$ and ii) commercially available compounds which are used as pigments or for other industrial applications: HgI_2, $Hg(CN)_2$, $HgCl_2O_8{\cdot}H_2O$, $Hg(SCN)_2$, HgF_2, $Hg_2(NO_3)_2{\cdot}H_2O$, $Hg(NO_3)_2{\cdot}2H_2O$. These compounds were included in the study for use as fingerprints.

In order to detect any potential interferences or interactions resulting from the thermal release of different Hg species, several mixtures of these Hg compounds were analysed. Due to the lack of standard reference materials for the analysis, the mixtures of Hg species were prepared in the laboratory. Mixtures of pure compounds were prepared by crushing 10 mg of each compound with silica to obtain blends with mercury concentrations of about 1000 mg kg^{-1}. It should be pointed that relatively high mercury concentrations are considered in this work to minimised heterogeneity problems. However the total mercury content of the analysed mixtures was kept to below 10µg to prevent the equipment from being contaminated. To procure the thermograms, approximately 5 mg of prepared mixture were used, depending on the Hg content. Quantification was carried out by peak integration using Origin 6.0 software.

3. Results and discussion

3.1. Mercury species identification: Pure compounds

Each Hg species was characterized by its thermo-desorption profile. The desorption profile shows the temperature at which thermal-release starts, reaches a maximum and returns to the baseline. The temperature at which maximal release was reached was considered as the peak temperature, being specific for each compound. The accuracy of the proposed method was tested by determining the average value of 10 replicate determinations of the desorption temperature for HgS red (Table 2). A well defined single peak with an intermediate desorption temperature was observed for this compound. The differences between the expected value and the result obtained being lower than 10%. This indicates a good accuracy of the results. The precision of the analysis was evaluated from the results of standard deviation (SD) and relative standard

deviations (%RSD). A good RSD value 6.6 % was achieved while SD value is relatively high (Table 2). This fact can be attributed to the low homogeneity obtained during the sample preparation in which a low quantity of standard is diluted with a proportionately high amount of silica.

The profiles obtained are shown in Fig. 1-4. As can be seen Hg halides present desorption peaks at the lowest temperatures (Fig. 1). The decomposition of $HgCl_2$ occurs at low temperatures, the maximum peak being 138 ºC. The high peak corresponding to Hg_2Cl_2 is at 119 ºC and exhibits a shoulder close to the peak temperature corresponding to $HgCl_2$. This shoulder is probably associated to the liberation of Hg_2Cl_2 [23].

The other Hg halides analyzed, HgI_2 and $HgBr_2$, have single peaks at approximately 100-110 ºC while the profile corresponding to HgF_2 moves to higher temperatures with two peaks at 234 and 450 ºC (Fig. 1). The peak at 450 ºC is attributed to the total decomposition of HgF_2, while the peak at the lower temperature could be due to the decomposition of Hg compounds formed during the analysis such as Hg_2F_2, or HgFOH [30].

The desorption profiles obtained for the two forms of HgO, yellow and red, are shown in Fig. 2. A maximum peak appears at 471 ºC and 284 ºC and there are smaller peaks at about 308 ºC and 469ºC for red and yellow HgO respectively. Red HgO consists of well-defined crystalline prismatic particles approximately 2 μm in size, which appear to be fused together, to form round multiparticle aggregates around 20 μm in diameter. Yellow HgO consists of smaller particles of around 1 μm that have less well-defined shape and form smaller aggregates about 5 μm in size. The specific surface areas were 0.45 and 0.68 $m^2\ g^{-1}$ for the red and yellow HgO respectively as measured by N_2

adsorption (BET method). The smaller peak may be due the secondary decomposition of oxide (I) Hg_2O during the analysis (1):

$$Hg_2O\ (s) \rightarrow 2Hg\ (g) + O\ (g) \qquad (1)$$

The Hg_2O forms at low temperatures (< 230 ºC) as a result of the oxidation of the free atoms of Hg by atomic oxygen at the interface between the two solid phases (HgO/Hg2O). Its formation is associated, with the formation of a reaction interface that separates the two solid phases (HgO/Hg_2O), and with the partial transfer of Hg_2O formation energy to the reactant, which enhances the decomposition of HgO (2) [28].

$$HgO\ (s) + Hg\ (g) + O\ (g) \qquad (2)$$

It should be noted that in the case of yellow HgO, the two peaks have a similar intensity. This can be attributed to the fact that the yellow form of HgO is more reactive than the red form due to the smaller particle size and therefore higher specific surface of the yellow form. Its decomposition occurs more rapidly in this compound whereas the other mercury oxides undergo a change in their internal structure due to the rise in temperature before the total release of mercury.

The desorption profiles corresponding to the S-containing mercury compounds are shown in Fig. 3. Red HgS decomposes in one step at 305 ºC according to the chemical equation (3) whereas $HgSO_4$ decomposes at a higher temperature, 583 ºC.

$$HgS\ (s) \rightarrow Hg\ (g) + \tfrac{1}{2}\ S_2\ (g) \qquad (3)$$

Hg_2SO_4 undergoes a two-step decomposition, with one peak appearing at approximately 300ºC and a second peak at 514 ºC slightly displaced from the HgSO4 decomposition area. The presence of two intense peaks in the desorption profile suggests that the thermal decomposition of Hg_2SO_4 takes place via reactions 4, 5 and 6. Equations 5 and

6 describe the thermal decomposition of $HgSO_4$ and of the unstable intermediate product $HgSO_4 \cdot 2HgO$ [29].

$$Hg_2SO_4\ (s) \rightarrow HgSO_4\ (s) + Hg\ (g) \quad (4)$$

$$3\ HgSO_4\ (s) \rightarrow HgSO_4 \cdot 2HgO\ (s) + 2\ SO_2\ (g) + O_2\ (g) \quad (5)$$

$$HgSO_4 \cdot 2HgO\ (s) \rightarrow 3Hg\ (g) + SO_2\ (g) + 2O_2\ (g) \quad (6)$$

The desorption profiles of the N-containing mercury compounds are shown in Fig. 4. The thermal desorption of the mercury nitrates (I) and (II) is reflected in two peaks, a first peak at 264-280 ºC and a second peak at 450 ºC, probably related to the decomposition of mercury nitrates in HgO which occur between 400-500 ºC (7-9). However, it must be taken into account that mercury (I) nitrate exhibits reducing properties. It is partially oxidized by atmospheric oxygen at ambient temperatures forming mercury nitrate (II) and mercury (9) so in its decomposition also could appears $Hg(NO_3)_2$.

$$Hg(NO_3)_2\ (s) \rightarrow HgO\ (s) + N_2O_5\ (g) \quad (7)$$

$$Hg_2(NO_3)_2\ (s) \rightarrow 2HgO\ (s) + 2NO2 \quad (8)$$

$$Hg_2(NO_3)_2\ (s) \rightarrow Hg(NO_3)_2\ (s) + Hg \quad (9)$$

As can be seen in Figure 4 the peaks in the desorption profiles of the mercury nitrates (I) and (II) are in similar position but the peak corresponding to the decomposition of HgO (at 450 ºC) is more intense in the profile of nitrate mercury (I) because its decomposition is generating more HgO.

The $Hg(CN)_2$ decomposition profile presents a broad peak at 267 ºC. The thermal decomposition profile of $Hg(SCN)_2$ presents two peaks, an intense peak at about 177 ºC

and a small peak at 288 ºC close to the position of red HgS (305±12ºC) probably related to the decomposition of $Hg(SCN)_2$ in HgS as a result of the thermal analysis (pharaoh serpent reaction) (10).

$$2Hg(SCN)_2\ (s) \rightarrow 2HgS\ (s) + CS_2\ (aq) + C_3N_4(s) \qquad (10)$$

The desorption profile of mercury (II) perchlorate hydrate is shown in Fig. 5. The desorption of $Hg(ClO_4)_2 \cdot H_2O$ presents an intense peak at about 273 ºC and two smaller peaks at 475 and 590 ºC. The thermal decomposition of this compound could occur via reactions (11) and (12), decomposing either to form either the chloride and oxygen or the oxide and mixtures of chlorine and oxygen.

$$Hg(ClO_4)_2\ (s) \rightarrow HgCl_2\ (s) + 2O_2\ (g) \qquad (11)$$

$$Hg(ClO_4)_2\ (s) \rightarrow HgO\ (s) + Cl_2\ (g) + O_2\ (g) \qquad (12)$$

Table 3 summarises the characteristic peak temperatures of each compound. These compounds are used as a reference.

3.2. Mercury species identification: Mixtures of pure compounds

In order to evaluate possible interferences or interactions during the thermal release of the different mercury species, several Hg compound mixtures were analysed. The results obtained (Fig. 6) confirm that different mercury species can be identified in a sample. No important interferences were observed when $HgCl_2$:$HgSO_4$; $HgCl_2$:HgS(red) and $HgCl_2$:$Hg(NO_3)_2 \cdot H_2O$:$HgSO_4$ were tested (Fig. 6a-c). A slight deviation in the case of $HgSO_4$ was observed in the mixtures HgO:$HgSO_4$ and $HgCl_2$:HgO:$HgSO_4$ (Fig. 6d-e). In these two mixtures the maximum peak for $HgSO_4$ appears at a lower temperature. This suggests that an interaction between these

compounds occurs. The mechanism of interaction is probably that represented in eq. (5-6).

3.3. Verification of the method

Due to the lack of reference materials for Hg species, red HgS, was used to verify the proposed method. Its thermal decomposition profile is shown in Fig. 3. Only one peak is produced, so the total mercury concentration obtained from calculation of the peak area (experimental) should fit the expected concentration. Table 4 shows the results obtained for the analysis of 5 sample replicates. Recoveries in the range of 79-104 % were estimated suggesting that the method may be explored for quantitative purposes.

4. Conclusions

These results show thermal decomposition to be a promising technique for determining mercury speciation in solid samples. Good accuracy of the results was obtained. The differences between the expected value and the result obtained being lower than 10%. A good RSD value 6,6 % was achieved while SD value is relatively high. This fact can be attributed to the low homogeneity obtained during the sample preparation.

The results show it is possible to identify the mercury species from their temperature of decomposition. The temperature decomposition rate of the mercury species was arranged in increasing order as follows: HgI_2<$HgBr_2$<Hg_2Cl_2=$HgCl_2$<$Hg(CN)_2$< $HgCl_2O_8{\cdot}H_2O$< $Hg(SCN)_2$< HgS (red)< HgF_2< $Hg_2(NO_3)_2{\cdot}2H2O$< $Hg(NO_3)_2{\cdot}H_2O$< HgO (yellow, red) < Hg_2SO_4< $HgSO_4$.

No important interferences were observed in the mixtures tested, apart from slight deviations when $HgSO_4$ and HgO were present together in a sample. This fact is attributed to the formation of an intermediate compound.

Acknowledgements

This work was financed by the PCTI Asturias, the European Regional Development Fund in Asturias (FEDER 2007-2013) and HUNOSA through the project PC10-20. We would like to acknowledge the support of CSIC for providing M. Rumayor with a JAE-Predoc fellowship and M.A. Lopez-Anton with a JAE-Doc contract (European Social Fund)

Literature

[1] Pirrone, N., Cinnirella, S., Feng, X., Finkelman, R. B., Friedli, H. R., Leaner, J., Mason, R., Mukherjee, A. B., Stracher, G. B., Streets, D. G., Telmer, K., Global mercury emissions to the atmosphere from anthropogenic and natural sources, Atmos. Chem. Phys. 10 (2010) 5951-5964.

[2] UNEP Global Mercury assessment 2013. Published by UNEP, 2013. Available online at http://www.unep.org/PDF/PressReleases/GlobalMercuryAssessment2013.pdf.

[3] Kolker, A., Senior, C. L., Quick, J. C., Mercury in coal and the impact of coal quality on mercury emission from combustion systems, Appl. Geochem. 21 (2006) 1821-1836.

[4] Pavlish, J. H., Hamre, L. L., Zhuang, Y., Mercury control technologies for coal combustion and gasification systems, Fuel 89 (2010) 838-847.

[5] N.S. Bloom, E. Preus, Proceedings of the 2nd International Symposium on Contaminated Sediments, 2003, pp.331–336.

[6] R. Fernández-Martínez, M.I. Rucandio, Anal.Bioanal.Chem. 375 (2003) 1089–1096.

[7] N.W. Revis, T.R. Osborne, D. Sedgley, A. King, Analyst 114 (1989) 823–825.

[8] H. Sakamoto, T. Tomiyasu, N. Yonehara, Anal.Sci. 8 (1992) 35–39.

[9] R. Rubio, G. Rauret, J. Radioanal. Nucl. Chem. 208 (1996) 529–540.

[10] J.R. Bacon, C.M. Davidson, nalyst 133 (2008) 25–46.

[11] A.T. Reis, S.M. Rodrigues, C.M. Davidson, E. Pereira, A.C. Duarte, Chemosphere 81 (2010) 1369–1377.

[12] C.S. Kim, G.E. Brown, J.J. Rytuba, Sci. Total Environ. 261 (2000) 157–168.

[13] C.S. Kim, J.J. Rytuba, G.E. Brown, J. Colloid Interface Sci. 271 (2004) 1–15.

[14] C.S. Kim, .S. Bloom, J.J. Rytuba, G.E. Brown, Environ. Sci. Technol. 37 (2003) 5102–5108.

[15] H.Biester, M. Gosar, G. Müller, J. Geochem. Explor. 65 (1999) 195–204.

[16] H. Biester, G. Nehrke, J. Fresenius, Anal. Chem. 358 (1997) 446–452.

[17] A. Bollen, A. Wenke, H. Biester, Water Res. 42 (2008) 91–100.

[18] H. Biester, C. Scholz, Environ. Sci. Technol. 31 (1997) 233–239.

[19] Biester, H.; Gosar, M.; Covelli, S. Environ. Sci. Technol. 2000, 34, 3330-3336.

[20] Olga V. Shuvaeva, Maria A. Gustaytis, Gennadii N. Anoshin, Analytica Chimica Acta 6 2 1 (2 0 0 8) 148–154.

[21] A.T. Reis, J.P.Coelho, S.M.Rodrigues, R.Rocha, C.M.Davidson, A.C.Duarte, E. Pereira, Talanta 2012, 99, 363-638.

[22] M. Ozaki, Md.A Uddin, E. Sasaoka, S. Wub. Fuel 87 (2008) 3610–3615

[23] C. Raposo, C.C. Windmöller, W.A.D Júnior. Waste Manage. 23 (2003) 879–886

[24] X. Feng, J.Y. Lu, D.C. Gregoire, Y. Hao, C.M. Banic, W.H. Schroeder. Bioanal Chem (2004) 380: 683–689

[25] J. Li, Y. Yuan, R. Perry, M.M. Maroto-Valer. Prepr. Pap.-Am. Chem. Soc., Div. Fuel Chem. 52 (2) (2007) 511–512

[26] M. Rallo, M.A. Lopez-Anton, R. Perry, M.M. Maroto-Valer. Fuel 89 (2010) 2157–2159

[27] M.A. Lopez-Anton, Yang Y, R. Perry, M.M Maroto-Valer. Fuel 89 (2010) 629–634

[28] B. V. L'vov, Thermochimica Acta 333 (1999) 21-26

[29] S. A. Tariq and J. O. Hill, Journal of Thermal Analysis 21 (1981) 277–281

[30] B. Brunetti, V. Piacente, A. Latini, P. Scardala, J. Chem. Eng. Data 2008, 53, 2493–2495

Figure captions

Fig 1. Thermal-desorption profiles of the Hg-halides.

Fig. 2. Thermal-desorption profiles of the mercury oxides.

Fig. 3. Thermal-desorption profiles of the S-containing mercury compounds.

Fig. 4. Thermal-desorption profiles of the N-containing mercury compounds.

Fig. 5. Thermal-desorption profiles of mercury(II) perchlorate hydrate.

Fig. 6. Thermal-desorption profiles of the mixtures: (a) $HgCl_2$:$HgSO_4$(1:1); (b) $HgCl_2$:HgSred(1:1); (c) $HgCl_2$:$Hg(NO_3)_2 \cdot H_2O$:$HgSO_4$(1:1:1); (d) HgOred:$HgSO_4$(1:1) and (e) $HgCl_2$:HgOred:$HgSO_4$(1:1:1).

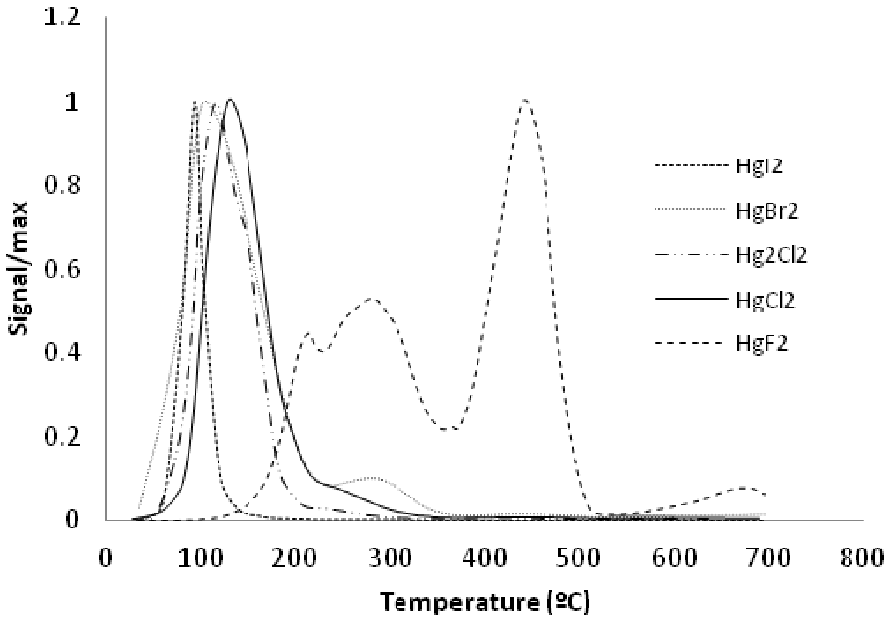
1.2
1
0.8
0.6
0.4
0.2
0
Signal/max
0
100
200
300
400
500
600
700
800
Temperature (ºC)
HgI2
HgBr2
Hg2Cl2
HgCl2
HgF2

Fig 1.

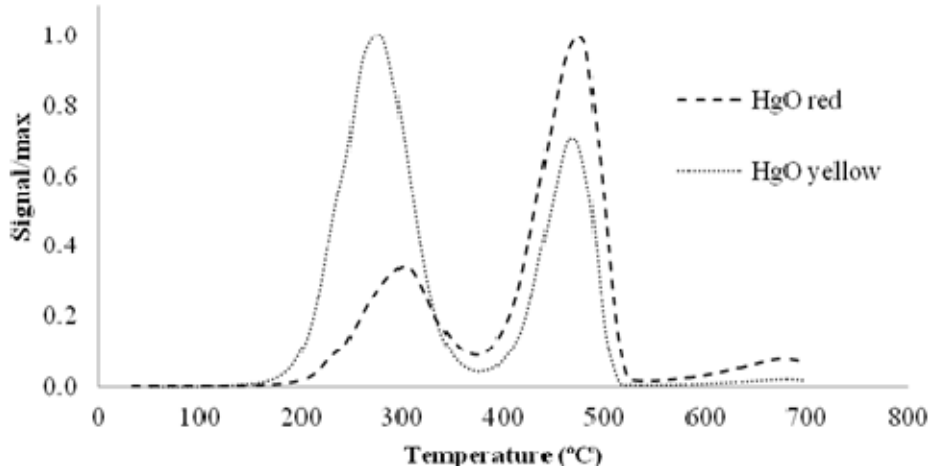
1.0
0.8
0.6
0.4
0.2
0.0
Signal/max
0
100
200
300
400
500
600
700
800
Temperature (°C)
HgO red
HgO yellow

Fig. 2.

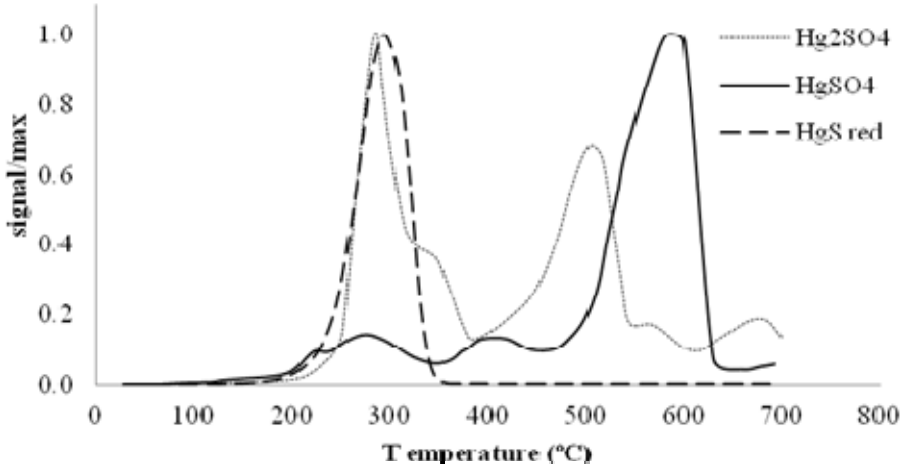
1.0
0.8
0.6
0.4
0.2
0.0
signal/max
0
100
200
300
400
500
600
700
800
Temperature (°C)
Hg2SO4
HgSO4
HgS red

Fig. 3.

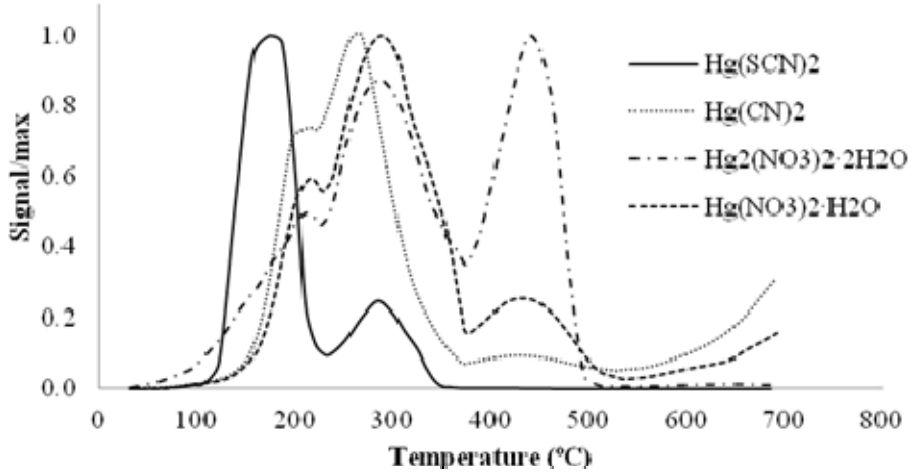
1.0
0.8
0.6
0.4
0.2
0.0
Signal/max
0
100
200
300
400
500
600
700
800
Temperature (°C)
Hg(SCN)2
Hg(CN)2
Hg2(NO3)2·2H2O
Hg(NO3)2·H2O

Fig. 4.

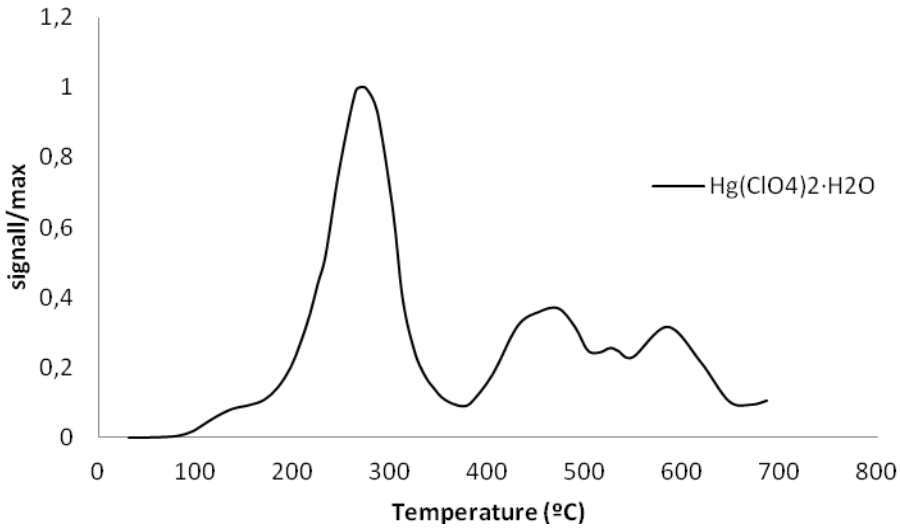
1,2
1
0,8
0,6
0,4
0,2
0
signall/max
0
100
200
300
400
500
600
700
800
Temperature (ºC)
Hg(ClO4)2·H2O

Fig. 5.

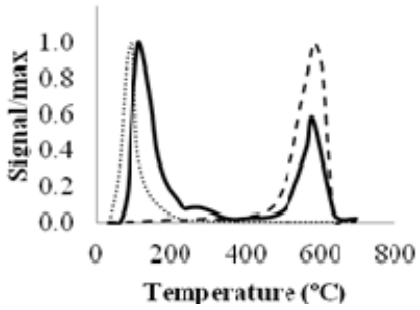
Signal/max
1.0
0.8
0.6
0.4
0.2
0.0
0
200
400
600
800
Temperature (°C)

(a)

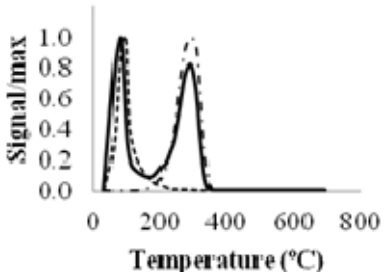
Signal/max
1.0
0.8
0.6
0.4
0.2
0.0
0
200
400
600
800
Temperature (°C)

(b)

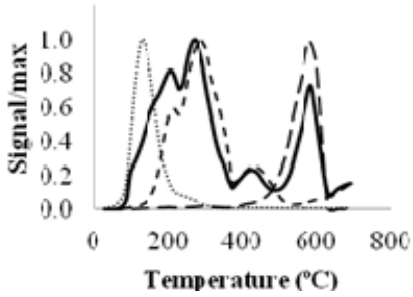
Signal/max
1.0
0.8
0.6
0.4
0.2
0.0
0
200
400
600
800
Temperature (°C)

(c)

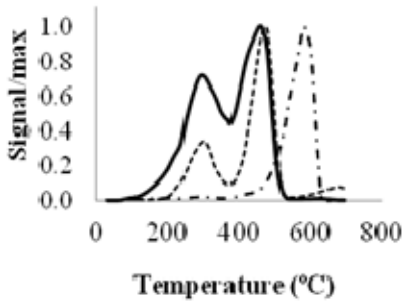
Signal/max
1.0
0.8
0.6
0.4
0.2
0.0
0
200
400
600
800
Temperature (°C)

(d)

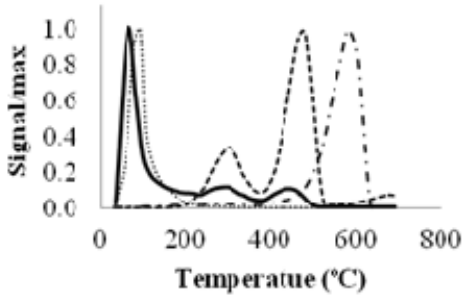
Signal/max
1.0
0.8
0.6
0.4
0.2
0.0
0
200
400
600
800
Temperatue (°C)

(e)

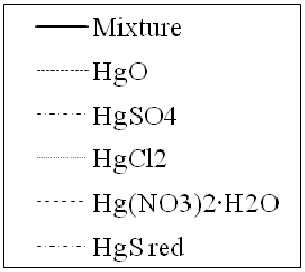
Mixture
HgO
HgSO4
HgCl2
Hg(NO3)2·H2O
HgSred

Fig. 6.

Table 1. Heating program optimised for the analysis.

Time (s)	**Heating rate (ºC/min)**
0-575	40
576-775	50
776-900	80

Table 2. Validation results obtained for HgS red analysed by thermo-desorption technique. [Hg]=744 $mg \cdot Kg^{-1}$

Sample	[Hg] ($mg \cdot Kg^{-1}$)
1	836
2	809
3	836
4	757
5	769
6	769
7	729
8	779
9	696
10	707
X ($mg \cdot Kg^{-1}$)	765
SD_{tot}	51
RSD (%)	6.6

Table 3. Thermal dissociation temperatures corresponding to the pure mercury compounds.

Mercury compounds	High peak T (ºC)	Start T- End T decomposition peak (ºC)
HgI_2	100±12	60-180
$HgBr_2$	110±9	60-220
Hg_2Cl_2	119±9	60-250
$HgCl_2$	138±4	90-350
HgS red	305±12	210-340
HgF_2	234±42; 449±12	120-350; 400-500
HgO red	308±1; 471±5	200-360; 370-530
HgO yellow	284±7; 469±6	190-380;320-540
Hg_2SO_4	295±4; 514±4	200-400;410-600
$HgSO_4$	583±8	500-600
$Hg(SCN)_2$	177±4; 288±4	100-220; 250-340
$Hg(CN)_2$	267±1	140-360
$Hg(NO_3)_2{\cdot}H_2O$	215±4; 280±13; 460±25	150-370; 375-520
$Hg_2(NO_3)_2{\cdot}2H_2O$	264±35; 427±19	120-375; 376-500
$HgCl_2O_8{\cdot}H_2O$	273±1;475±5; 590±9	154-360;380-510;520-650

Table 4. Comparison of expected and obtained Hg concentrations and recovery values for 5 replicates of red HgS analyzed by means of the thermo-desorption technique.

Replicate	[Hg]theor.[1] ($mg \cdot kg^{-1}$)	[Hg]est.[2] ($mg \cdot kg^{-1}$)	Recovery (%)
1	979	776	79
2	428	382	89
3	390	405	104
4	506	414	82
5	392	310	79